Further characterization of the interaction between the cytoskeletal proteins talin and vinculin

Mark D. BASS, Bipin PATEL, Igor G. BARSUKOV, Ian J. FILLINGHAM, Robert MASON, Beverley J. SMITH, Clive R. BAGSHAW and David R. CRITCHLEY[1]
Department of Biochemistry, University of Leicester, University Road, Leicester LE1 7RH, U.K.

The cytoskeletal protein talin, which is thought to couple integrins to F-actin, contains three binding sites (VBS1–VBS3) for vinculin, a protein implicated in the negative regulation of cell motility and whose activity is modulated by an intramolecular interaction between the vinculin head (Vh) and vinculin tail (Vt) domains. In the present study we show that recombinant talin polypeptides containing the three VBSs (VBS1, residues 498–636; VBS2, residues 727–965; and VBS3, residues 1943–2157) each bind tightly to the same or overlapping sites within vinculin$_{1-258}$. A short synthetic talin VBS3 peptide (residues 1944–1969) was sufficient to inhibit binding of a ^{125}I-labelled talin VBS3 poly-peptide to vinculin$_{1-258}$, and NMR spectroscopy confirmed that this peptide forms a 1:1 complex in slow exchange with vinculin$_{1-258}$. Binding of the ^{125}I-labelled VBS3 polypeptide was

markedly temperature dependent, but was not inhibited by 1 M salt or 10 % (v/v) 2-methyl-2-propanol. Attempts to further define the talin-binding site within vinculin$_{1-258}$ using a gel-blot assay were unsuccessful, but near maximal talin-binding activity was retained by a construct spanning vinculin residues 1–131 in a yeast two-hybrid assay. Interestingly, the talin VBS3 poly-peptide was a potent inhibitor of the Vh–Vt interaction, and the VBS3 synthetic peptide was able to expose the actin-binding site in intact vinculin, which is otherwise masked by the Vh–Vt interaction. The results suggest that under certain conditions, talin may be an effective activator of vinculin.

Key words: actin, α-catenin, focal adhesions, integrins.

INTRODUCTION

Talin is a 270 kDa cytoskeletal protein which is thought to link the cytoplasmic domain of the integrin family of adhesion receptors to the actin cytoskeleton [1]. It is an elongated (60 nm) flexible protein [2], which is suggested to exist as an antiparallel dimer at concentrations above 0.7 mg/ml [3,4]. The N-terminal region of talin (residues 1–433), which can be liberated as a globular monomeric 50 kDa polypeptide by calpain II cleavage [5], contains two potential membrane anchors (residues 21–39 and 385–406) [6], plus a FERM domain (residues 86–410; where FERM stands for band 4.1/ezrin/radixin/moesin) [7]. The FERM domain contains binding sites for the cytoplasmic do-mains of β1A, β1D [8] and β3 [9] integrin subunits, as well as the C-type lectin layilin [10], the protein tyrosine kinase focal adhesion kinase (FAK) [10] and F-actin [11]. The talin rod, which is dimeric [12] and comprises approx. 60 alanine-rich repeats [13], contains a second integrin-binding site [14], and a highly conserved C-terminal actin-binding site (residues 2345–2541) [11], which is homologous to that found in the actin-binding proteins Sla2p and Hip-1 [11,15]. Therefore talin has the potential to link integrins directly to the actin cytoskeleton. The talin rod also contains three binding sites for the cytoskeletal protein vinculin [16,17], which has multiple binding partners [α-actinin, α-catenin, vasodilator-stimulated phosphoprotein (VASP), vinexin, ponsin, paxillin and F-actin], and whose activity is regulated by PtdIns(4,5)P_2 [1,18].

The role of talin in cell adhesion has been explored using a variety of techniques. Inactivation of talin in neuronal growth cones using chromophore-assisted laser inactivation inhibits filopodial extension [19], and the talin homologue filopodin is localized at the tips of filopodia in *Dictyostelium discoideum* [20].

In fibroblasts, talin co-localizes with layilin in membrane ruffles [10] and with integrins in cellular junctions with the extracellular matrix (focal adhesions) [21], and microinjection of talin anti-bodies leads to the disruption of focal adhesions and associated actin stress fibres [22,23]. Similar results were obtained following microinjection of the recombinant talin FERM domain and a polypeptide containing both the C-terminal vinculin-binding site (VBS) and actin-binding site [11]. Down-regulation of talin expression in HeLa cells decreased the rate of cell spreading and led to a reduction in the size of focal adhesions [24], although some of this effect appeared to be indirect and was due to altered integrin processing [25]. Similarly, mouse em-bryonic stem cells, in which both copies of the talin gene were disrupted, showed spreading defects and were unable to assemble focal adhesions [26]. In mice, talin knockout arrests development at gastrulation probably due to a failure of mesoderm migration [27]. Altogether, these observations are consistent with the idea that talin plays a key role in coupling integrins to the actomyosin contractile apparatus in the cell.

In contrast, cells in which the vinculin gene has been disrupted can still assemble focal adhesions, although the cells spread less well and show reduced adhesion to fibronectin [28,29]. However, vinculin $(-/-)$ cells are more motile and show higher levels of tyrosine phosphorylation of proteins such as FAK, p130Cas and paxillin, which are known to be important in cell motility [29]. These observations suggest that vinculin negatively regulates cell motility, and this may explain why it behaves as a tumour suppressor in model systems [30]. How vinculin exerts these effects is presently unclear. Possibilities include a role for vinculin in stabilizing focal adhesions by cross-linking an integrin–talin complex either to F-actin or to the membrane [1]; the vinculin tail (Vt) can bind to PtdIns(4,5)P_2 and has been shown to insert

---

into the lipid bilayer [31]. Alternatively, vinculin may act by sequestering PtdIns(4,5)P_2 from phosphoinositide 3-kinase preventing synthesis of PtdIns(3,4,5)P_3, a pathway implicated in the remodelling of focal adhesions induced by platelet-derived growth factor [32]. Finally, it may be significant that the paxillin-binding site in vinculin is constitutively active [33], whereas most of the other ligand binding sites in vinculin are masked by an intramolecular interaction between the vinculin head (Vh) and Vt [34] which is relieved by PtdIns(4,5)P_2 [33,35]. This raises the possibility that vinculin might negatively regulate cell motility by sequestering paxillin, which is implicated in focal adhesion signalling [36]. Interestingly, paxillin and vinculin co-localize in the perinuclear region in serum-starved Swiss 3T3 cells which lack focal adhesions, and the ADP-ribosylation factor-1 GTPase drives paxillin (but not vinculin) out of this region into small focal adhesion-like structures [37].

As part of an effort to further define the role of talin and vinculin in integrin-mediated cell adhesion, we have used the yeast two-hybrid system to map the VBSs in talin to three short peptide sequences 25–30 residues in length and spanning talin residues 607–636, 852–876 and 1944–1969 (referred to as VBS1–3 respectively) [17]. The sites are 59 % similar, although only two residues are completely conserved, and are predicted to form amphipathic helices. In the present study, we report the biochemical characterization of these sites and show that each binds to the same site in vinculin with high affinity. We also show that a talin polypeptide containing VBS3 competes with the C-terminal Vt for binding to vinculin residues 1–258, although the binding sites for VBS3 and Vt show distinctive features.

MATERIALS AND METHODS

Expression of recombinant talin and vinculin polypeptides

The plasmid constructs used for expression of chicken talin and vinculin polypeptides in *Escherichia coli* were generated by PCR using primers that contained unique restriction sites, which allowed the PCR products to be cloned directionally into either the *Nde*I/*Bam*HI sites of pET-15b (Novagen, Cambridge Bioscience, Cambridge, U.K.) or the *Eco*RI/*Bam*HI sites of pGEX-2T (Amersham Biosciences, Little Chalfont, Bucks., U.K.). The following Bluescript constructs were used as templates; pBS54A, 23B and GG4A which encode chicken talin residues 102–656, 642–1328 and 1646–2541 respectively [16]; and pBS2.89 kb and pBScVin5 which encode chicken vinculin residues 1–881 and 1–1066(Δ167–207) respectively [38]. Recombinant polypeptides were expressed in the BL21(DE3) strain of *E. coli*. Glutathione S-transferase (GST) fusion proteins were purified using GSH–agarose beads and His-tagged polypeptides were purified using a nickel ion-chelating column following standard procedures. The concentrations of recombinant polypeptides were determined using the Coomassie Plus Protein Assay® (Pierce, Rockford, IL, U.S.A.).

Purification of native talin, vinculin and actin

Talin [39] and vinculin [40] were purified from turkey gizzard smooth muscle. Actin was isolated from rabbit skeletal muscle as described by Spudich and Watt [41], and was further purified by gel-filtration using a Superdex-200 column (Amersham Biosciences).

Iodination of proteins

Aliquots of protein (100 μl; 40 μg) in 100 mM potassium phosphate buffer (pH 7.5) containing 150 mM NaCl were labelled (for 30 min) to a specific radioactivity of approx. 3×10^6 c.p.m./

μg by the addition of 100 μCi of [^{125}I]NaI (ICN Biomedicals, Irvine, CA, U.S.A.) in the presence of *N*-chloro-benzenesulphonamide immobilized on polystyrene beads (Pierce). Labelled protein was purified on a PD10 de-salting column (Amersham Biosciences) using the same buffer containing 0.25 % gelatin and 0.01 % sodium azide.

Biotinylation of polypeptides

A His-tagged talin polypeptide spanning residues 1943–2157 (VBS3) was biotinylated as follows; 35 μg/ml sulphosuccinimidyl-6-(biotinamido)-hexanoate (Pierce) was added to 0.75 mg/ml VBS3 in PBS [160 mM Na_2HPO_4, 30 mM KH_2PO_4 (pH 7.4), 140 mM NaCl and 3 mM KCl] and incubated at 4 °C for 30 min. To stop the reaction 100 mM Tris/HCl (pH 8.0) was then added, and the labelled VBS3 was dialysed into 50 mM Tris/HCl (pH 8.0)/150 mM NaCl.

Binding of labelled talin polypeptides to vinculin fusion proteins

Binding of ^{125}I-labelled or biotinylated talin polypeptides to a GST–vinculin$_{1-258}$ fusion protein was determined using either a pull-down or a gel-blot assay. In the pull-down assay, up to 170 pmol of GST–vinculin$_{1-258}$ was immobilized on GSH–agarose beads and mixed with the appropriate ^{125}I-labelled talin polypeptide in 500 μl of buffer P [60 mM imidazole, 0.8 mM Tris/HCl (pH 7.3), 190 mM NaCl, 2 mM EGTA, 5 mM dithiothreitol and 0.2 % haemoglobin] for various time periods. The beads were then washed twice with the same buffer, and the amount of bound ligand was determined using a γ-radiation counter. The free ligand concentration in the assay was calculated from the concentration of ligand in the first wash. By the nature of this assay, only sites with slow kinetics ($k_{off} < 0.01$ s^{-1}) will be detected. The amount of GST–vinculin bound to the beads was quantified by Western-blot analysis using an anti-GST antibody (Santa Cruz Biotechnology, Santa Cruz, CA, U.S.A.) followed by scanning densitometry. The effective concentration of the vinculin on the beads was not accurately known, but the values quoted refer to the values if the amount was distributed homogeneously in the assay volume. In order to maximize the fraction of labelled talin bound, the concentration of vinculin was greater than the K_d for talin binding in most assays. As a result the observed IC$_{50}$ value for a competing peptide equals $K_d + ([\text{vinculin}]/2)$, and is dominated by the latter term for high affinity interactions (i.e. $K_d < 350$ nM).

In the gel-blot assay, *E. coli* expressing the GST–vinculin fusion proteins were lysed and the proteins were resolved by SDS/PAGE and then transferred on to nitrocellulose. The blot was blocked with 25 mM Tris/HCl (pH 7.5), 150 mM NaCl, 1 % (v/v) Tween 20 and 4 % (w/v) BSA for 2 h at 20 °C, and then overlaid with 10 ng/ml biotinylated VBS3 in blocking buffer for 10 h at 4 °C. The blot was washed with the same buffer for 1 h at 20 °C, overlaid with steptavidin–horseradish peroxidase (Amersham Biosciences) diluted 1:5000 in blocking buffer, and bound VBS3 was detected using an ECL® kit.

Actin co-sedimentation assay

Vinculin (0.5 μM) was incubated overnight with 5 μM G-actin and a synthetic talin VBS3 peptide (0–500 μM) in buffer A [2 mM Tris/HCl (pH 8.0), 0.2 mM $CaCl_2$, 0.2 mM Na_2ATP and 0.5 mM 2-mercaptoethanol]. Actin polymerization was initiated by the addition of 2 mM $MgCl_2$/100 mM KCl and was allowed to proceed for 2 h at 20 °C. F-actin was sedimented through a 20 % (w/v) sucrose cushion at 440000 *g* for 1 h and proteins

present in the pellet and the supernatant were analysed by SDS/PAGE followed by staining with Coomassie Brilliant Blue.

Analysis of the talin-binding site in vinculin using the yeast two-hybrid assay

Chicken vinculin polypeptides were expressed as fusion proteins with the yeast LexA DNA-binding domain using the vector pBTM116. Each of the three VBSs in chicken talin were expressed as fusion proteins with the GAL4 transactivation domain using the vector pGAD GH (ClonTech Laboratories). The sequence of each construct was confirmed by automated DNA sequencing. Plasmids were transformed into the L40 strain of *Saccharomyces cerevisiae*, and positive interactions were identified using a quantitative β-galactosidase assay as described previously [17].

Analysis of the vinculin–talin interaction by NMR spectroscopy

His-tagged vinculin$_{1-258}$ was expressed in *E. coli*, and purified using a 1-ml HiTrap chelating affinity column charged with nickel sulphate (Amersham Biosciences). The protein was dialysed against 50 mM Tris/HCl (pH 8.0)/150 mM NaCl, and the protein concentration was determined using the Coomassie Plus Protein Assay® (Pierce). The His-tag was then removed by cleavage with 1 unit of human plasma thrombin (Roche Diagnostics) per 10 mg of protein (4 h at 20 °C), and the protein was dialysed into 20 mM Tris/HCl (pH 8.0)/10 mM NaCl. The liberated vinculin polypeptide was then purified to homogeneity on a 1-ml HiTrap Q Sepharose column (Amersham Biosciences) using a 100 ml linear NaCl gradient (10 mM to 1 M NaCl). Binding of non-tagged vinculin$_{1-258}$ (2 mg/ml) to increasing concentrations of a synthetic talin peptide (stock solution of 0.9 mg/ml) containing a minimal VBS (residues 1944–1969) was analysed by NMR spectroscopy in 20 mM Tris/HCl (pH 7.5)/10 mM NaCl. A truncated version of this peptide (residues 1955–1969) was used as a control (stock solution of 0.45 mg/ml). Spectra were recorded at 25 °C on a Bruker DRX600 spectrometer using the WATERGATE water suppression method [42] in combination with the water-flip-back technique [43]. The Tris signal was attenuated by low-power presaturation in relaxation delay.

RESULTS AND DISCUSSION

The three VBSs in talin show similar characteristics

We have previously shown that there are three non-overlapping VBSs (VBS1–3) in talin that show 59 % similarity to each other [17]. To characterize these binding sites in more detail, we initially assayed binding of a recombinant ^{125}I-labelled talin polypeptide (residues 1943–2157) containing VBS3 to a GST–vinculin$_{1-258}$ fusion protein which contains the talin-binding site. Binding of ^{125}I-labelled VBS3 increased in proportion to the amount of GST–vinculin immobilized on the beads, and there was little binding to GST alone (results not shown). Binding of ^{125}I-labelled VBS3 was saturable (Figure 1A) with an estimated K_d of approx. 39 nM. This value is similar to that reported for the interaction between intact ^{125}I-labelled vinculin and talin [16,34]. Binding could also be readily detected using the unlabelled VBS3 polypeptide and analysis of bound material by SDS/PAGE (Figure 1B), consistent with tight binding.

Binding of ^{125}I-labelled VBS3 to GST–vinculin was progressivly inhibited by increasing concentrations of unlabelled VBS3 (either with or without the His-tag) as well as unlabelled VBS1 (residues 498–636) and VBS2 (residues 727–965), whereas a His-tagged talin polypeptide (residues 2270–2541) which contains the C-terminal actin-binding site [11] failed to inhibit binding (results
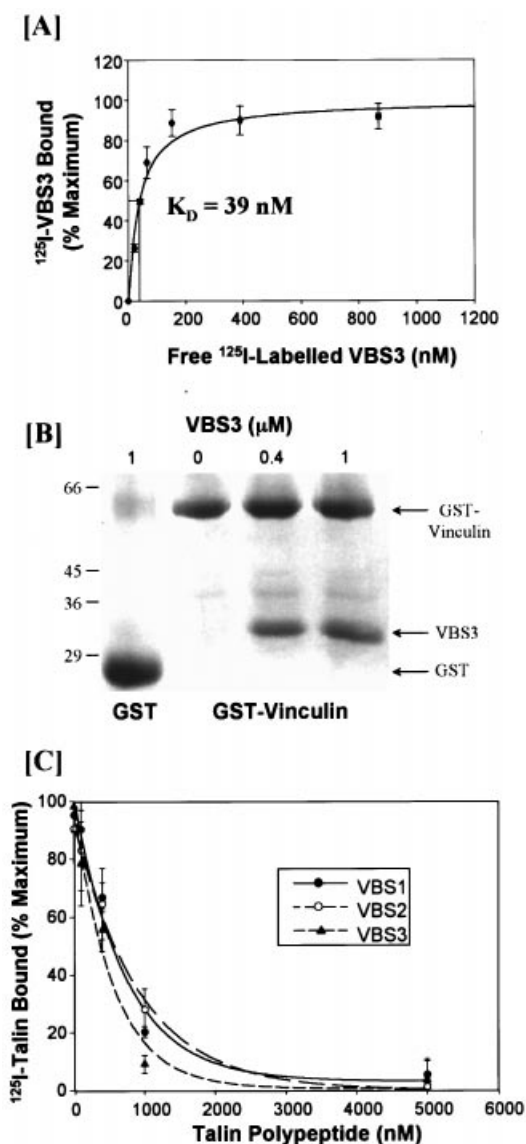

Figure 1   Binding of a talin VBS3 polypeptide to GST–vinculin

(**A**) Increasing concentrations of His-tagged ^{125}I-labelled VBS3 polypeptide (residues 1943–2157) were incubated (for 3 h at 19 °C) with a GST–vinculin$_{1-258}$ fusion protein (50 pmol; effective concentration of approx. 100 nM) immobilized on GSH–agarose beads, and suspended in 500 μl of buffer P (see the Materials and methods section). Unbound material was removed by washing. A plot of the amount of bound against free ^{125}I-labelled VBS3 (determined from the first wash) showed that binding was saturable, with an estimated K_d of 39 nM. The experiment was repeated four times and bars represent S.E.M. (**B**) Unlabelled talin VBS3 polypeptide (0.4 or 1 μM) was incubated with GST–vinculin$_{1-258}$ immobilized on GSH–agarose beads for 20 min at 4 °C, and bound VBS3 was analysed by SDS/PAGE and visualized by staining the gel with Coomassie Brilliant Blue. Molecular mass markers (kDa) are shown to the left of the Figure. (**C**) ^{125}I-labelled talin (20 nM) was incubated (for 20 min at 4 °C) with GST–vinculin$_{1-258}$ immobilized on GSH–agarose beads (170 pmol; effective concentration of approx. 350 nM) in the presence of increasing concentrations of unlabelled talin VBS1 (residues 498–636), VBS2 (residues 727–965) and VBS3 (residues 1943–2157) polypeptides. Similar concentrations of each of the talin polypeptides (VBS1–3) quantitatively inhibited talin binding. The experiments were repeated four times and bars represent S.E.M. Note that under these conditions, the IC$_{50}$ is dominated by the [vinculin] term (see the Materials and methods section).

not shown). The results indicate that all three sites in talin interact with the same region in vinculin. If this is correct, then each of the three talin VBS polypeptides should quantitatively inhibit binding of intact ^{125}I-labelled talin to the GST–vinculin$_{1-258}$ fusion protein, and the results shown in Figure 1(C) confirm that
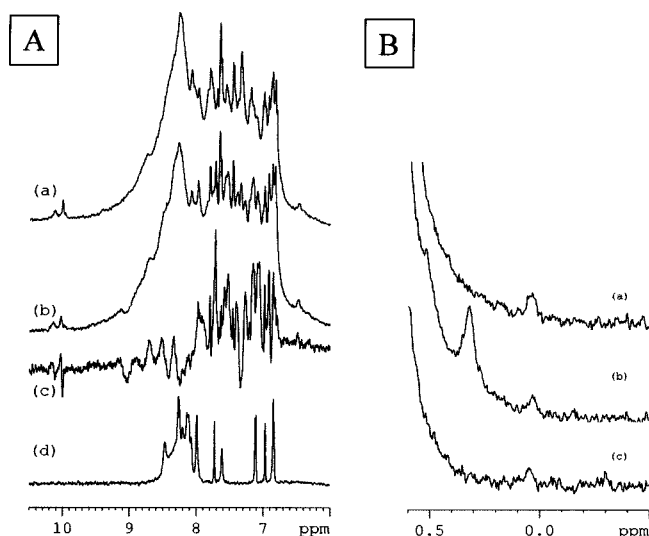
Figure 2   Changes in ¹H NMR spectra of vinculin$_{1-258}$ upon addition of a synthetic talin VBS3 peptide

(**A**) Changes in ¹H NMR spectra of vinculin$_{1-258}$ upon addition of a minimal synthetic talin VBS3 peptide (residues 1944–1969; single-letter code, YTKKELIESARKVSEKVSHVLAALQA). Low-field regions of (a) free vinculin$_{1-258}$; (b) an equimolar mixture of vinculin$_{1-258}$ and the minimal VBS3 peptide; and (c) difference spectrum i.e. spectrum (a) subtracted from spectrum (b). Positive resonances correspond to the signals of the complex not present in the spectrum of the free protein. These are either peptide signals or protein signals that change position upon complex formation. The negative signals correspond to the signals of the free protein that change position upon complex formation. The spectrum of the free VBS3 peptide is shown in (d). (**B**) High-field region of ¹H NMR spectra of (a) free vinculin$_{1-258}$; (b) equimolar mixture of vinculin$_{1-258}$ and the minimal VBS3 peptide; and (c) equimolar mixture of vinculin$_{1-258}$ and the truncated VBS3 peptide (residues 1955–1969). Please note the change in the vertical scale.

this was indeed the case. Although VBS1–3 appear to have similar biochemical properties, sequence comparisons show that only two residues, a leucine and an alanine, are totally conserved across all three sites [17]. Comparison of each site from human to nematodes identifies a series of totally conserved, predominantly hydrophobic, residues characteristic of each site that we assume defines the protein fold.

A short synthetic talin VBS3 peptide can bind to vinculin

Using a yeast two-hybrid approach, each of the VBSs in talin has been defined to a sequence of approx. 25–30 amino acids [17]. To investigate whether such a short talin peptide can bind to vinculin *in vitro*, the ability of a minimal VBS3 synthetic peptide to inhibit binding of recombinant ¹²⁵I-labelled VBS3 (residues 1943–2157) to GST–vinculin$_{1-258}$ was evaluated. The results showed that a talin VBS3 peptide spanning residues 1944–1969 did indeed inhit binding, whereas a truncated version of this peptide spanning residues 1955–1969 was unable to do so (results not shown).

Binding of the minimal talin VBS3 peptide to vinculin$_{1-258}$ was further assessed by NMR spectroscopy. The addition of the VBS3 peptide resulted in significant changes in the NMR spectrum (Figure 2A), which were most apparent in the difference spectrum (Figure 2A, spectrum c). Complex formation is indicated by the change in chemical shift of some of the protein resonances upon addition of the VBS3 peptide, as well as from the difference between resonances of the peptide free in solution and in the presence of vinculin$_{1-258}$. The latter is particularly easy to observe from the comparison of the difference spectrum in

Figure 2(A) (spectrum c) with that of the free peptide in Figure 2(A) (spectrum d). However, when vinculin$_{1-258}$ was titrated with the truncated VBS3 peptide, the difference spectrum at all peptide concentrations showed only resonances of the free peptide, and no indication of changes in the protein spectrum (results not shown). From these results we conclude that vinculin$_{1-258}$ binds to the VBS3 peptide, whereas there is no interaction with the truncated peptide. The intensities of the signals in the difference spectrum depend linearly upon the VBS3 peptide concentration until an equimolar ratio of vinculin$_{1-258}$ to VBS3 peptide is reached. After that, a new set of sharp signals appears corresponding to the signals of the free peptide, and no further changes in the broad signals are detected. The resonances of the complex showed no concentration-dependent broadening or chemical shift changes (results not shown). The spectral changes are clearly visible in the high-field region of the spectrum (Figure 2B). Here the spectrum of the complex (Figure 2B, spectrum b) has an additional resonance at 0.32 p.p.m., not observed in the spectrum of the free protein (Figure 2B, spectrum a), that allowed us to monitor complex formation. The intensity of the resonance corresponds to that of a methyl group, and the low chemical shift is most likely the effect of an aromatic ring proximity. All observed spectral changes agree with the formation of a 1:1 peptide–protein complex in slow exchange on the NMR time-scale. The overall changes in the NMR spectra upon complex formation are restricted to a relatively small number of signals, as is evident from the difference spectrum of Figure 2(A) (spectrum c). This indicates that the proton environment change upon peptide binding is restricted to the binding site and that no large conformational changes occur.

Characterization of the nature of the vinculin–talin interaction

Binding of the ¹²⁵I-labelled VBS3 talin polypeptide to GST–vinculin$_{1-258}$ immobilized on GSH–agarose beads was slow at 4 °C [time to reach half-maximal binding ($t_{1/2}$) = 131 min], and the amount bound at equilibrium could be reduced to approx. 30% of maximum by the addition of 600 nM unlabelled VBS2 (Figure 3A). Raising the temperature to 19 and 37 °C markedly increased the rate of binding ($t_{1/2}$ = 17 and 13 min respectively). The elution of bound ¹²⁵I-labelled VBS3 at 4 °C was also slow ($t_{1/2}$ = 172 min), and although raising the temperature to 19 °C did increase the rate of dissociation (Figure 3B), the effect was not as dramatic as that seen for binding. This indicates that as the temperature is increased, the association rate constant increases relative to the dissociation rate constant, i.e. the affinity increases with increasing temperature. The slow time course for ¹²⁵I-labelled VBS3 binding to and release from the Vh fragment suggests that the interaction is multistep.

The three VBSs in talin are each predicted to form short amphipathic helices containing approx. 21 residues [17]. Vinculin residues 1–258 are also predicted to contain a series of amphipathic helices, but the chemical nature of the interaction between the two proteins has not been determined. Talin VBS1 contains three leucine residues (Leu⁶⁰⁸, Leu⁶¹⁵ and Leu⁶²²) that align down one side of the helix, which might form a potential leucine zipper [17]. However, in VBS2 one of the leucine residues is replaced by a methionine, and in VBS3 two of the leucine residues are replaced by valine residues. Single point mutations of the conserved leucine residues in VBS1 to alanine did not reduce binding to vinculin residues 1–258, as determined using a yeast two-hybrid assay. While a double leucine (Leu⁶⁰⁸/Leu⁶²²) mutant showed a marked reduction in binding, the residual binding activity was still quite high. Analysis of binding of the minimal talin VBS3 peptide to GST–vinculin by NMR spectroscopy
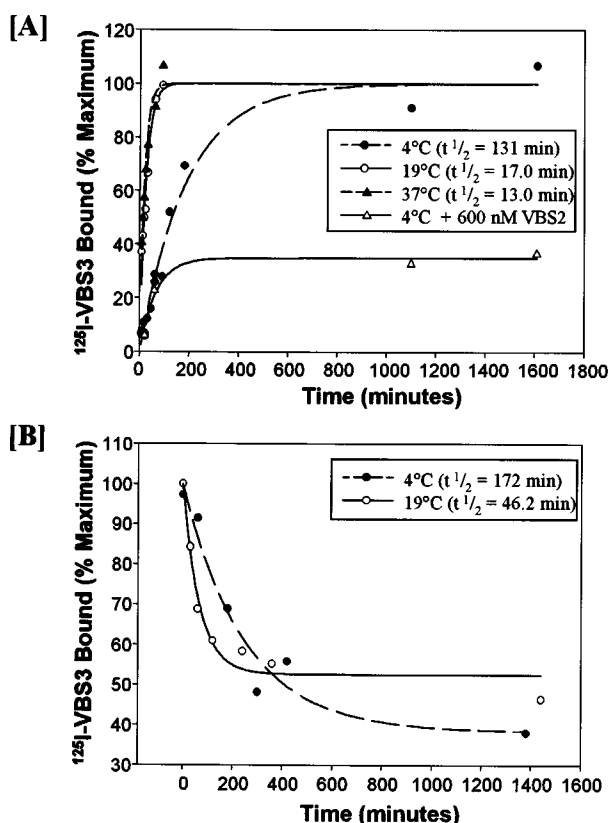
[A]

[B]

Figure 3 ¹²⁵I-labelled talin VBS3 binding to and dissociation from GST–vinculin

(**A**) ¹²⁵I-labelled VBS3 (20 nM) was incubated with GST–vinculin$_{1-258}$ immobilized on GSH–agarose beads at 4, 19 or 37 °C for various times, before removing unbound material by washing. The amount of ¹²⁵I-labelled VBS3 bound was determined using a γ-radiation counter. Binding was also determined in the presence of 600 nM unlabelled VBS2 polypeptide to determine binding specificity. Under these conditions, binding was limited to approx. 30 % of the maximum. Each of these results was reproduced on 2–4 separate occasions. (**B**) ¹²⁵I-labelled VBS3 was bound to GST–vinculin$_{1-258}$ for 21 h before washing away unbound material. The dissociation of ¹²⁵I-labelled VBS3 was followed over time in the presence of 5 μM unlabelled VBS3 at both 4 and 19 °C. Each of these results was reproduced on 2–4 separate occasions.

suggests close contacts between aromatic and aliphatic residues in the complex. However, the alcohol 2-methyl-2-propanol, which is a potent inhibitor of hydrophobic interactions [44], failed to inhibit binding of ¹²⁵I-labelled VBS3 to GST–vinculin$_{1-258}$ at concentrations up to 10 % (results not shown).

Each of the VBSs in talin is basic (pI values of approx. 9.1), but single point mutations of conserved basic residues (Lys¹⁹⁴⁷, Arg¹⁹⁵⁴ and Lys¹⁹⁵⁹) in VBS3 to alanine (or a Lys¹⁹⁴⁷/Arg¹⁹⁵⁴ double mutation) had no effect on binding to vinculin$_{1-258}$ in a yeast two-hybrid assay (results not shown). Similarly, salt concentrations up to 1 M had no effect on binding of the ¹²⁵I-labelled VBS3 polypeptide to GST–vinculin$_{1-258}$ (results not shown). We conclude that binding of vinculin to talin is not solely determined by either hydrophobic or electrostatic interactions.

Further characterization of the talin-binding site in the Vh

We have previously mapped the talin-binding site in the Vh to residues 1–258 using both gel-blot and solid-phase assays [45]. However, attempts to further define this site by introducing

N-terminal deletions have failed using both *in vitro* binding [45] and yeast two-hybrid assays [17]. The recently determined structure of the N-terminal region of α-catenin [46], which is homologous to vinculin, provides insights into the possible structure of this region of vinculin. α-Catenin residues 82–262 comprise five helices that form two distinct substructures. Helix 1 runs antiparallel to the first half of the long helix 2, and the C-terminal part of helix 2 forms part of an antiparallel four-helix bundle with helices 3–5. Since the core hydrophobic residues of α-catenin are totally conserved in vinculin, along with the proline residues that introduce a kink into helices 3 and 4, it seems likely that vinculin residues 70–247 will adopt a similar fold. A structure for the complex between α-catenin and its ligand β-catenin has also been solved [46]. This shows that residues 59–82 of α-catenin (equivalent to residues 40–63 of vinculin) are also helical (helix 0), and again the core hydrophobic residues are conserved in vinculin. Helices 0, 1 and the N-terminal part of the long helix 2 pack against a short helix from β-catenin (residues 121–141) involving both polar and apolar contacts, i.e. three helices in α-catenin bind to a short helix in β-catenin. It is interesting that vinculin also interacts with a short peptide sequence in talin that is predicted to be helical [17], and it is tempting to speculate that vinculin residues 40 (predicted start of helix 0) to part way through long helix 2 (predicted to end at residue 147) contain the talin-binding site.

To investigate this possibility, we expressed a series of deletion mutants based on the GST–vinculin$_{1-258}$ construct where the C-terminal boundary was designed according to the α-catenin structure. Talin binding was assayed using biotinylated VBS3 and an SDS gel-blot assay. In agreement with previous results, GST–vinculin$_{1-258}$ retained talin-binding activity in this assay [44], but a deletion which removed residues 215–258 (predicted helix 5) completely abolished binding (Figure 4A). Identical results were obtained when binding was assayed to purified GST–vinculin$_{1-214}$ immobilized in microtitre wells (results not shown). However, we have previously obtained different results using the yeast two-hybrid assay. Thus a LexA fusion protein containing vinculin residues 1–167 supported binding to each of the three VBSs in talin just as well as the 1–258 construct, while deletion of residues 1–57 almost completely destroyed binding [17]. We therefore tested the ability of vinculin residues 1–131 to bind to talin VBS3 in the yeast two-hybrid assay. The results showed that it retained approx. 70 % activity of the control vinculin$_{1-258}$ construct (Figure 4B).

The difference in the results obtained using the two assays is illustrated by point mutations in the highly conserved sequence Arg¹⁷⁸-Gln-Gln-Glu¹⁸¹. GST–vinculin$_{1-398}$ fusion proteins bearing an Arg¹⁷⁸ → Glu or a Glu¹⁸¹ → Lys mutation, were unable to bind talin *in vitro* (Glu¹⁸¹ → Asp behaved as wild-type) [45], whereas the Glu¹⁸¹ → Lys mutation had no major effect on the binding of a vinculin$_{1-258}$ construct to talin VBS1–3 in the yeast two-hybrid assay (Figure 4C). It is interesting to note that there is an identical Arg-Gln-Gln-Glu sequence in all vertebrate α-catenins, which is located at the end of helix 3 and is part of the antiparallel four-helix bundle [46]. Presumably, this region is essential to the overall protein fold, and mutations therein may reduce the affinity of GST–vinculin for talin VBS3 such that binding can no longer be detected in assays which include extensive washing steps. In the yeast two-hybrid assay, the components do not undergo physical separation, and therefore this method is probably better at detecting lower affinity binding interactions. In conclusion, the results from the yeast two-hybrid experiments strongly indicate that the talin-binding site in vinculin is contained within residues 1–131. Whether the interaction is mediated in a similar way to the α-catenin–β-catenin
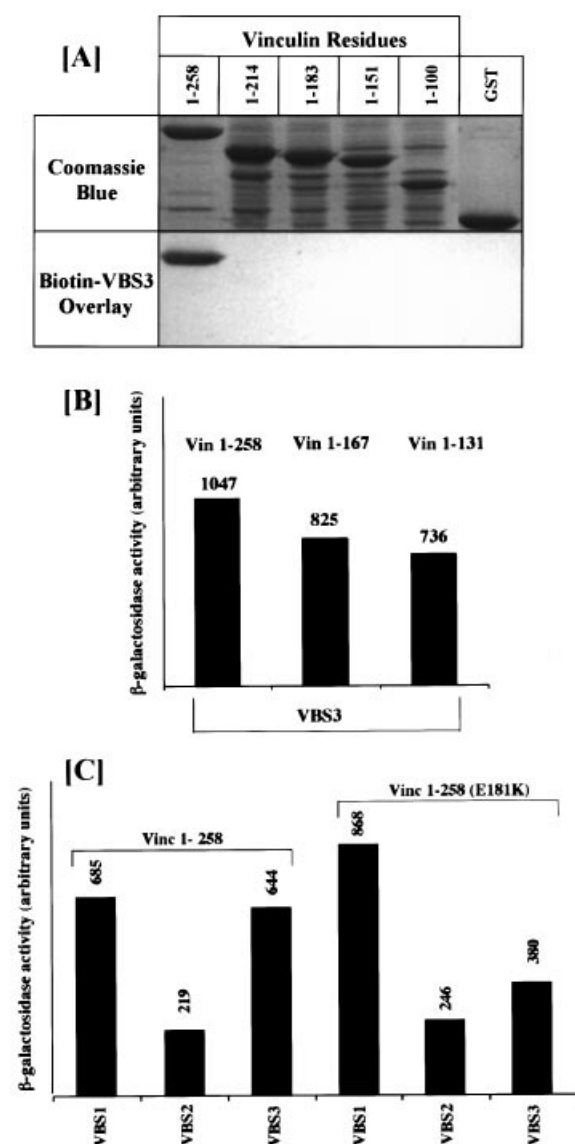
Figure 4   Identification of the talin-binding site in vinculin using *in vitro* binding and yeast two-hybrid assays

(**A**) The series of GST–vinculin fusion proteins shown were expressed in *E. coli*, resolved by SDS/PAGE and transferred on to nitrocellulose. The blot was overlaid with 10 ng/ml biotinylated-VBS3 for 10 h at 4 °C, washed and then bound VBS3 was detected with streptavidin–horseradish peroxidase and an ECL® kit. VBS3 bound specifically to GST–vinculin$_{1–258}$, but failed to interact with any of the truncated polypeptides. This result was reproduced on two separate occasions. (**B** and **C**) Talin polypeptides spanning VBS1 (residues 498–636), VBS2 (residues 727–965) and VBS3 (residues 1943–2157) expressed in yeast as GAL4 transactivation domain fusion proteins were tested for binding to vinculin residues 1–258, and mutants thereof expressed as Lex A DNA-binding domain fusion proteins. Interaction between the talin and vinculin polypeptides was monitored by assaying β-galactosidase activity (arbitrary units) in yeast cell lysates. Activity values are shown above each column, and are the means of duplicate determinations. The experiments were repeated at least three times with essentially the same result. Lamin–Lex A and Byr2–GAL4 fusion proteins were used as negative controls, and the interaction between Ras–Lex A and Byr2–GAL4 was used as a positive control (results not shown). Vin(c), vinculin.

interaction [46] awaits the determination of the structure of the complex.

Does the Vt bind to the same site in vinculin as talin?

In intact vinculin, an intramolecular interaction between Vh and Vt obscures the binding sites for talin [34] and α-actinin [47] in
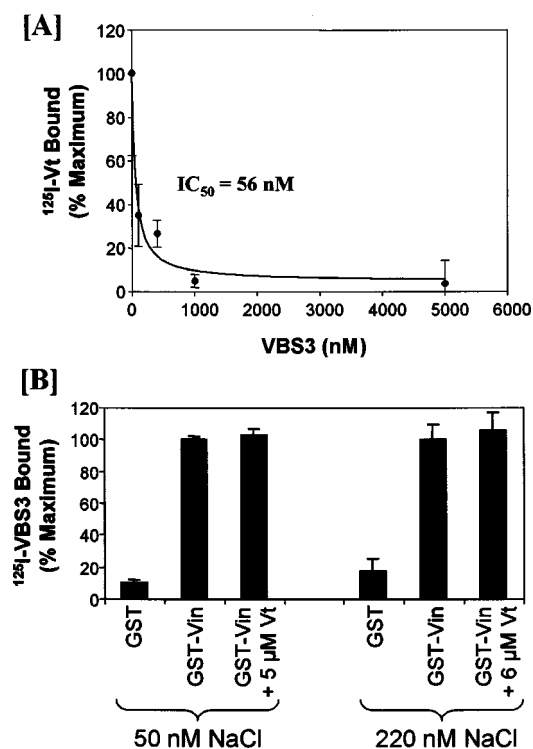
Figure 5   Recombinant Vt polypeptide binds to GST–vinculin$_{1–258}$ with lower affinity than talin VBS3

(**A**) ^{125}I-labelled Vt (residues 878–1066) (80 nM) was incubated (for 3 h at 19 °C) in 500 μl of buffer P (see the Materials and methods section) with GST–vinculin$_{1–258}$ (50 pmol; effective concentration of approx. 100 nM) immobilized on GSH–agarose beads, and in the presence of increasing amounts of unlabelled talin VBS3. Unbound material was removed by washing, and the amount of ^{125}I-labelled Vt bound was determined using a γ-radiation counter. ^{125}I-labelled Vt binding was progressively inhibited by increasing concentrations of unlabelled VBS3 with an IC_{50} value of approx. 56 nM. This experiment was repeated four times and bars represent S.E.M. (**B**) Binding of ^{125}I-labelled VBS3 (20 nM) to GST–vinculin$_{1–258}$ was not inhibited by unlabelled Vt even when used at concentrations as high as 6 μM. Since binding of Vt has been reported to be markedly reduced at NaCl concentrations > 100 mM [49], the experiment was conducted in both 50 and 220 mM NaCl. These experiments were repeated four times and bars represent the S.E.M. Vt minus the His-tag was prepared as described previously [50]. Vin, vinculin.

Vh, and for F-actin in Vt [48]. This suggests that either Vt and talin bind to the same site in Vh, or that Vt sterically inhibits binding of talin. To explore these possibilities, we tested the ability of Vt and VBS3 to compete for binding to GST–vinculin$_{1–258}$ immobilized on GSH–agarose beads. Unlabelled VBS3 was an effective inhibitor of ^{125}I-labelled Vt binding with an IC_{50} of 56 nM (Figure 5A). In contrast, binding of ^{125}I-labelled VBS3 (20 nM) to GST–vinculin$_{1–258}$ was not inhibited by concentrations of unlabelled Vt as high as 6 μM (Figure 5B). This is surprising given that the K_d value for the interaction between Vt and Vh has been estimated to be between 50 nM [34] and 93 nM [49], and is therefore in the same range as the vinculin–talin interaction [16,34]. Miller et al. [49] have recently shown that the binding of Vt to a GST fusion protein containing vinculin residues 1–266 is markedly reduced by salt concentrations above 100 mM. Since the above experiments were conducted in 190 mM salt, we repeated the experiment in 50 and 220 mM salt. However, Vt (5 μM) again failed to inhibit binding of VBS3 to GST–vinculin$_{1–258}$ (Figure 5B).

We have previously shown that Vt binds to sequences within vinculin residues 1–258 [35], and recent studies by others indicate
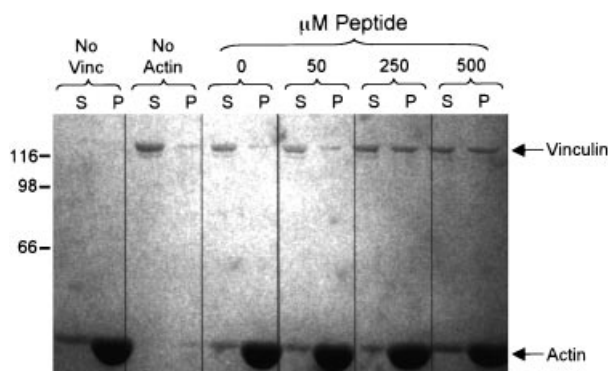
Figure 6   Native vinculin can be activated by a talin VBS3 synthetic peptide

Vinculin (0.5 μM) purified from turkey gizzard smooth muscle was preincubated overnight in buffer A (see the Materials and methods section) with increasing concentrations of a synthetic talin VBS3 peptide (residues 1944–1969) containing a minimal VBS. G-actin (5 μM) was added and polymerization was initiated by the addition of 2 mM $MgCl_2$/100 mM KCl. The F-actin was sedimented at 440 000 *g* through a 20% (w/v) sucrose cushion, and vinculin present in the pellet (P) and supernatant (S) was analysed by SDS/PAGE followed by staining with Coomassie Brilliant Blue. Molecular mass markers (kDa) are shown to the left of the Figure. In the absence of the talin peptide, vinculin failed to bind to F-actin, whereas addition of of 250–500 μM peptide resulted in approx. 50% of the vinculin co-sedimenting with F-actin. This result was reproduced on five separate occasions. Vinc, vinculin.

that residues 181–226 are sufficient for Vt binding [49]. The pI of this region is 8.16, suggesting that this basic region in Vh might bind via electrostatic interaction to an acidic region in Vt. The recently determined crystal structure of Vt reveals a cleft flanked by acidic residues Asp^{1013}, Glu^{1014} and Glu^{1015} at the top of a five-helix bundle, which was predicted to bind Vh [50]. Mutation of these residues to alanine has now been shown to abolish the interaction of Vt with GST–$vinculin_{1-266}$ [49]. Moreover, the fact that Vt binding to Vh is inhibited by increasing salt concentrations confirms that electrostatic interactions are major binding determinants. Therefore, although both talin and Vt bind to the N-terminal region of vinculin, the nature of the interaction is clearly different, since binding of talin is not salt sensitive. The yeast two-hybrid data presented in the current study suggest that talin binds to vinculin residues 1–131, whereas Vt binds to residues 181–226 [49]. The mechanism by which Vt obscures the talin binding site therefore requires consideration. Interestingly, Vt residues 940–960, which form part of helix 3 and contain a ladder of basic residues [50], show 64%, 55% and 45% similarity with talin VBS1–3 respectively. Perhaps the acidic patch at the top of the Vt five-helix bundle initially binds to Vh residues 181–226, which carry a net positive charge, and the basic ladder on Vt helix 3 then interacts with and obscures the talin-binding site in Vh (residues 1–131), which has a net negative charge (pI = 4.56).

VBS3 peptide can activate vinculin

The intramolecular interaction between Vh and Vt can be relieved by PtdIns(4,5)P_2 [33,35], exposing the talin and α-actinin binding sites in Vh and the VASP binding site in the proline-rich domain [51]. However, PtdIns(4,5)P_2 appears to mask the F-actin binding site in Vt [52], and, perhaps significantly, the binding sites for PtdIns(4,5)P_2 [31] and F-actin [53,54] in Vt partially overlap. This suggests that vinculin activated by PtdIns(4,5)P_2 on the cytoplasmic face of the plasma membrane may be able to bind talin or α-actinin, but not F-actin. Whether vinculin can be

activated by other mechanisms remains to be investigated. The *Shigella* protein IpaA has been shown to bind with high affinity ($K_d = 5$ nM) to the talin-binding site within Vh exposing the F-actin binding site in Vt [55]. Similarly, a vinculin-binding peptide isolated by phage display, and which shows some similarity to talin VBS3 [56], inhibited binding of Vh to Vt, and exposed the F-actin binding site in Vt [52]. To investigate whether authentic talin VBS3 can also activate vinculin, the effect of a VBS3 synthetic peptide on the ability of vinculin to bind F-actin was assessed using a co-sedimentation assay. Vinculin isolated from turkey gizzard binds poorly to F-actin, and > 80% of the protein remained unbound in the supernatant. The addition of increasing concentrations of VBS3 peptide markedly enhanced the amount of vinculin that co-sedimented with F-actin (Figure 6), although the peptide did not cause vinculin to sediment in the absence of F-actin (results not shown). These results support the idea that talin can shift the equilibrium for vinculin from the closed to the open conformation.

However, previous studies have shown that although Vt was an effective inhibitor of talin binding to the Vh (IC_{50} of approx. 40 nM), talin only partially inhibited (approx. 50%) binding of the 95 kDa Vh to Vt [34]. Moreover, this level of inhibition was only achieved when talin and Vh were preincubated for 16 h. One possibility is that the VBSs in intact talin in solution are not maximally active, and that they are therefore less effective at competing with Vt for binding to Vh. It has been noted that vinculin binds more efficiently to the talin rod than intact talin [57]. Perhaps the VBSs in talin recruited to the cytoplasmic face of integrins are activated such that talin can now displace the Vh–Vt interaction. Interestingly, the integrin-binding site(s) in talin has recently been shown to be activated by PtdIns(4,5)P_2 [58].

REFERENCES

1   Critchley, D. R. (2000) Focal adhesions – the cytoskeletal connection. Curr. Opin. Cell Biol. **12**, 133–139

2   Winkler, J., Lunsdorf, H. and Jockusch, B. M. (1997) Energy-filtered electron microscopy reveals that talin is a highly flexible protein composed of a series of globular domains. Eur. J. Biochem. **243**, 430–436

3   Molony, L., McCaslin, D., Abernethy, J., Paschal, B. and Burridge, K. (1987) Properties of talin from chicken gizzard smooth muscle. J. Biol. Chem. **262**, 7790–7795

4   Isenberg, G. and Goldmann, W. H. (1998) Peptide-specific antibodies localise the major lipid binding sites of talin dimers to oppositely arranged N-terminal 47 kDa subdomains. FEBS Lett. **426**, 165–170

5   Rees, D. J., Ades, S. E., Singer, S. J. and Hynes, R. O. (1990) Sequence and domain structure of talin. Nature (London) **347**, 685–689

6   Seelig, A., Blatter, X. L., Frentzel, A. and Isenberg, G. (2000) Phospholipid binding of synthetic talin peptides provides evidence for an intrinsic membrane anchor of talin. J. Biol. Chem. **275**, 17954–17961

7   Hamada, K., Shimizu, T., Matsui, T., Tsukita, S., Tsukita, S. and Hakoshima, T. (2000) Structural basis of the membrane-targeting and unmasking mechanisms of the radixin FERM domain. EMBO J. **19**, 4449–4462

8   Pfaff, M., Liu, S., Erle, D. J. and Ginsberg, M. H. (1998) Integrin β cytoplasmic domains differentially bind to cytoskeletal proteins. J. Biol. Chem. **273**, 6104–6109

9   Knezevic, I., Leisner, T. M. and Lam, S. C.-T. (1996) Direct binding of the platelet integrin $\alpha IIb\beta3$ (GPIIb-IIIa) to talin. Evidence that interaction is mediated through the coplasmic domains of both αIIb and $\beta3$. J. Biol. Chem. **271**, 16416–16421

10   Borowsky, M. L. and Hynes, R. O. (1998) Layilin, a novel talin-binding transmembrane protein homologous with C-type lectins, is localized in membrane ruffles. J. Cell Biol. **143**, 429–442

11   Hemmings, L., Rees, D. J. G., Ohanian, V., Bolton, S. J., Gilmore, A. P., Patel, N., Priddle, H., Trevithick, J. E., Hynes, R. O. and Critchley, D. R. (1996) Talin contains three actin-binding sites each of which is adjacent to a vinculin-binding site. J. Cell Sci. **109**, 2715–2726

12   Muguruma, M., Nishimuta, S., Tomisaka, Y., Ito, T. and Matsumara, S. (1995) Organisation of the functional domains in membrane cytoskeletal protein talin. J. Biochem. (Tokyo) **117**, 1036–1042

13   McLachlan, A. D., Stewart, M., Hynes, R. O. and Rees, D. J. G. (1994) Analysis of repeated motifs in the talin rod. J. Mol. Biol. **235**, 1278–1290

14   Calderwood, D. A., Zent, R., Grant, R., Rees, D. J. G., Hynes, R. O. and Ginsburg, M. H. (1999) The talin head domain binds to integrin β subunit cytoplasmic tails and regulates integrin activation. J. Biol. Chem. **274**, 28071–28074

15   McCann, R. O. and Craig, S. W. (1999) Functional genomic analysis reveals the utility of the I/LWEQ module as a predictor of protein:actin interaction. Biochem. Biophys. Res. Commun. **266**, 135–140

16   Gilmore, A. P., Wood, C., Ohanian, V., Jackson, P., Patel, B., Rees, D. J. G., Hynes, R. O. and Critchley, D. R. (1993) The cytoskeletal protein talin contains at least two distinct vinculin binding domains. J. Cell Biol. **122**, 337–347

17   Bass, M. D., Smith, B. J., Prigent, S. A. and Critchley, D. R. (1999) Talin contains three similar vinculin-binding sites predicted to form an amphipathic helix. Biochem. J. **341**, 257–263

18   Jockusch, B. M. and Rudiger, M. (1996) Crosstalk between cell adhesion molecules: vinculin as a paradigm for regulation by conformation. Trends Cell Biol. **6**, 311–315

19   Sydor, A. M., Su, A. L., Wang, F.-S., Xu, A. and Jay, D. G. (1996) Talin and vinculin play distinct roles in filopodial motility in the neuronal growth cone. J. Cell Biol. **134**, 1197–1207

20   Kreitmeier, M., Gerisch, G., Heizer, C. and Muller-Taubenberger, A. (1995) A talin homologue of *Dictyostelium* rapidly assembles at the leading edge of cells in response to chemoattractant. J. Cell Biol. **129**, 179–188

21   Burridge, K. and Connell, L. (1983) A new protein of adhesion plaques and ruffling membranes. J. Cell Biol. **97**, 359–367

22   Nuckolls, G. H., Romer, L. H. and Burridge, K. (1992) Microinjection of antibodies against talin inhibits the spreading and migration of fibroblasts. J. Cell Sci. **102**, 753–762

23   Bolton, S. J., Barry, S. T., Mosley, H., Patel, B., Jockusch, B. M., Wilkinson, J. M. and Critchley, D. R. (1997) Monoclonal antibodies recognizing the N- and C-terminal regions of talin disrupt actin stress fibers when microinjected into human fibroblasts. Cell Motil. Cytoskeleton **36**, 363–376

24   Albiges-Rizo, C., Frachet, P. and Block, M. R. (1995) Down regulation of talin alters cell adhesion and the processing of the $\alpha 5 \beta 1$ integrin. J. Cell Sci. **108**, 3317–3329

25   Martel, V., Vignoud, L., Dupe, S., Frachet, P., Block, M. R. and Albiges-Rizo, C. (2000) Talin controls the exit of the integrin $\alpha 5 \beta 1$ from an early compartment of the secretory pathway. J. Cell Sci. **113**, 1951–1961

26   Priddle, H., Hemmings, L., Monkley, S., Woods, A., Patel, B., Sutton, D., Dunn, G. A., Zicha, D. and Critchley, D. R. (1998) Disruption of the talin gene compromises focal adhesion assembly in undifferentiated but not differentiated ES cells. J. Cell Biol. **142**, 1121–1133

27   Monkley, S. J., Zho, X.-H., Kinston, S. J., Giblett, S. M., Hemmings, L., Priddle, H., Brown, J. E., Pritchard, C. A., Critchley, D. R. and Fassler, R. (2000) Disruption of the talin gene arrests mouse development at the gastrulation stage. Dev. Dyn. **219**, 560–574

28   Volberg, T., Geiger, B., Kam, Z., Pankov, R., Simcha, I., Sabanay, H., Coll, J.-L., Adamson, E. and Ben-Ze'ev, A. (1995) Focal adhesion formation by F9 embryonal carcinoma cells after vinculin gene disruption. J. Cell Sci. **108**, 2253–2260

29   Xu, W., Baribault, H. and Adamson, E. D. (1998) Vinculin knockout results in heart and brain defects during embryonic development. Development (Cambridge, U.K.) **125**, 327–333

30   Rodriguez Fernandez, J. L., Geiger, B., Salomon, D., Sabanay, I., Zoller, M. and Ben-Ze'ev, A. (1992) Suppression of tumorigenicity in transformed cells after transfection with vinculin cDNA. J. Cell Biol. **119**, 427–438

31   Johnson, R. P., Niggli, V., Durrer, P. and Craig, S. W. (1998) A conserved motif in the tail domain of vinculin mediates association with and insertion into acidic phospholipid bilayers. Biochemistry **37**, 10211–10222

32   Greenwood, J. A., Theibert, A. B., Prestwich, G. D. and Murphy-Ullrich, J. E. (2000) Restructuring of focal adhesion plaques by PI 3-kinase: regulation by PtdIns(3,4,5)-P_3 binding to α-actinin. J. Cell Biol. **150**, 627–641

33   Gilmore, A. P. and Burridge, K. (1996) Regulation of vinculin binding to talin and actin by phosphatidylinositol 4,5-bisphosphate. Nature (London) **381**, 531–535

34   Johnson, R. P. and Craig, S. W. (1994) An intramolecular association between the head and tail domains of vinculin modulates talin binding. J. Biol. Chem. **269**, 12611–12619

35   Weekes, J., Barry, S. T. and Critchley, D. R. (1996) Acidic phospholipids inhibit the intramolecular association between the N- and C-terminal regions of vinculin, exposing actin-binding and protein kinase C phosphorylation sites. Biochem. J. **314**, 827–832

36   Turner, C. E. (2000) Paxillin and focal adhesion signalling. Nat. Cell Biol. **2**, E231–E236

37   Norman, J. C., Jones, D., Barry, S. T., Holt, M. R., Cockcroft, S. and Critchley, D. R. (1998) ARF1 mediates paxillin recruitment to focal adhesions and potentiates rho-stimulated stress fibre formation in intact and permeabilised Swiss 3T3 cells. J. Cell Biol. **143**, 1981–1995

38   Price, G. J., Jones, P., Davison, M. D., Patel, B., Bendori, R., Geiger, B. and Critchley, D. R. (1989) Primary sequence and domain structure of chicken vinculin. Biochem. J. **259**, 453–461

39   Schmidt, J. M., Zhang, J., Lee, H.-S., Stromer, M. H. and Robson, R. M. (1999) Interaction of talin with actin: sensitive modulation of filament crosslinking activity. Arch. Biochem. Biophys. **366**, 139–150

40   Evans, R. R., Robson, R. M. and Stromer, M. H. (1984) Properties of smooth-muscle vinculin. J. Biol. Chem. **259**, 3916–3924

41   Spudich, J. A. and Watt, S. (1971) The regulation of rabbit skeletal muscle contraction. I. Biochemical studies of the interaction of the tropomyosin-troponin complex with actin and the proteolytic fragments of myosin. J. Biol. Chem. **246**, 4866–4871

42   Piotto, M., Saudek, V. and Sklenar, V. (1992) Gradient-tailored excitation for single-quantum NMR-spectroscopy of aqueous solutions. J. Biomol. NMR **2**, 661–665

43   Grzesiek, S. and Bax, A. (1993) The importance of not saturating H_2O in protein NMR – application to sensitivity enhancement and NOE measurement. J. Am. Chem. Soc. **115**, 12593–12594

44   Cupane, A., Vitrano, E. and Cordone, L. (1986) Effect of organic co-solvents on the dimer-tetramer equilibrium of human haemoglobin. J. Mol. Biol. **189**, 343–351

45   Gilmore, A. P., Jackson, P., Waites, G. T. and Critchley, D. R. (1992) Further characterisation of the talin binding site in the cytoskeletal protein vinculin. J. Cell Sci. **103**, 719–731

46   Pokutta, S. and Weis, W. L. (2000) Structure of the dimerisation and β-catenin-binding region of α-catenin. Mol. Cell **5**, 533–543

47   Kroemker, M., Rudiger, A. H., Jockusch, B. M. and Rudiger, M. (1994) Intramolecular interactions in vinculin control α-actinin binding to the vinculin head. FEBS Lett. **355**, 259–262

48   Johnson, R. P. and Craig, S. W. (1995) F-actin binding site masked by the intramolecular association of vinculin head and tail domains. Nature (London) **373**, 261–264

49   Miller, G. J., Dunn, S. D. and Ball, E. H. (2001) Interaction of the N- and C-terminal domains of vinculin. Characterization and mapping studies. J. Biol. Chem. **276**, 11729–11734

50   Bakolitsa, C., de Pereda, J. M., Bagshaw, C. R., Critchley, D. R. and Liddington, R. C. (1999) Crystal structure of the vinculin tail suggests a pathway for activation. Cell (Cambridge, Mass.) **99**, 603–613

51   Huttelmaier, S., Mayboroda, O., Harbeck, B., Jarchau, T., Jockusch, B. M. and Rudiger, M. (1998) The interaction of the cell-contact proteins VASP and vinculin is regulated by phosphatidylinositol-4,5-bisphosphate. Curr. Biol. **8**, 479–488

52   Steimle, P. A., Hoffert, J. D., Adey, N. B. and Craig, S. W. (1999) Polyphosphoinositides inhibit the interaction of vinculin with actin filaments. J. Biol. Chem. **274**, 18414–18420

53   Menkel, A. R., Kroemker, M., Bubeck, P., Ronsiek, M., Nikolai, G. and Jockusch, B. M. (1994) Characterisation of an F-actin-binding domain in the cytoskeletal protein vinculin. J. Cell Biol. **126**, 1287–1298

54   Huttelmaier, S., Bubeck, P., Rudiger, M. and Jockusch, B. M. (1997) Characterisation of two F-actin-binding and oligomerisation sites in the cell-contact protein vinculin. Eur. J. Biochem. **247**, 1136–1142

55   Bourdet-Sicard, R., Rudiger, M., Jockusch, B. M., Gounon, P., Sansonetti, P. J. and Nhieu, G. T. V. (1999) Binding of the *Shigella* protein IpaA to vinculin induces F-actin depolymerisation. EMBO J. **18**, 5853–5862

56   Adey, N. B. and Kay, B. K. (1997) Isolation of peptides from phage-displayed random peptide libraries that interact with the talin-binding domain of vinculin. Biochem. J. **324**, 523–528

57   Burridge, K. and Mangeat, P. (1984) An interaction between vinculin and talin. Nature (London) **308**, 744–746

58   Martel, V., Racaud-Sultan, C., Dupe, S., Marie, C., Paulhe, F., Galmiche, A., Block, M. R. and Albiges-Rizo, C. (2001) Conformation, localization, and integrin binding of talin depend on its interaction with phosphoinositides. J. Biol. Chem. **276**, 21217–21227